Metal-free acceptorless decarbonylation of formic acid enabled by a liquid chemical looping strategy

Arnaud Imberdis, Guillaume Lefèvre, Thibault Cantat

Metal-free acceptorless decarbonylation of formic acid enabled by a liquid chemical looping strategy

Arnaud Imberdis, Guillaume Lefèvre and Thibault Cantat*[a]

Abstract: The selective decarbonylation of formic acid was achieved under metal-free conditions. Using a liquid chemical looping strategy, the thermodynamically favored dehydrogenation of formic acid was shutdown, yielding a pure stream of CO, with no H_2 or CO_2 contamination. The transformation involves a two-step sequence where methanol is used as a recyclable looping agent to yield methylformate, which is subsequently decomposed to carbon monoxide using alkoxides as catalysts.

Among C1 chemicals, formic acid (HCOOH, FA) is the focus of renewed interests as it is an important product in catalytic transformations related to the storage of sustainable energies. Recent efforts have indeed showed that HCOOH is a key intermediate in the hydrogenation of CO_2 to methanol and methane.[1] In addition, formic acid can be produced from the (photo)electrolysis of CO_2 or the hydrogenation of CO_2 and carbonates.[2a–c] Despite its simple formulation, FA can undergo different decomposition reactions, depending on the reaction conditions and the presence of catalysts. While homogeneous catalysts have appeared that can disproportionate FA to methanol, the main decomposition path involves the dehydrogenation of HCOOH to H_2 and CO_2.[3a–e] In fact, the reversible hydrogenation of CO_2 (and bicarbonates) to formates has led to the concept of a hydrogen battery, for the storage of H_2 in a liquid form.[4]

From a thermodynamic standpoint, FA could also decompose to CO and H_2O, with a Gibbs free energy of –12.4 kJ·mol^{-1} at 298 °C (Scheme 1).[5] This decarbonylation reaction is less favoured than the classical dehydrogenation (ΔG°= –32.9 kJ·mol^{-1} at 298 °C);[5] yet, it would provide a convenient flow of CO, from a renewable feedstock. Utilized in large scale in the Fischer-Tropsch and Cativa processes,[6] as well as in hydroformylation reactions, carbon monoxide is currently produced from fossil sources, for example primarily from methane steam reforming (SMR) or autothermal reformer (ATR).[7] Alternatively, the Reverse Water Gas Shift (RWGS) reaction can convert CO_2 and H_2 to a mixture of CO, H_2O, CO_2 and H_2, at equilibrium.[8] Overall, these methods suffer from severe disadvantages, such as the need for further purification of the gas stream, to separate CO. In this context, the production of CO from FA would afford an attractive way to produce a stream of pure CO, in a controlled way, from a sustainable and storable precursor.[9]

Examples of the in situ decomposition of formic acid to promote for example formal carbonylation or hydroxycarbonylation have been reported.[10] Only several methods have been developed to promote the acceptorless decarbonylation of FA, which relied on the use of stoichiometric amounts of sulfuric or phosphoric acids[11] or on thermolytic conditions.[12] Catalytic strategies are scarce. They involve zeolite-based catalysts able to decompose FA at high temperatures (> 150 °C), to remove water, and exhibit modest activities with turnover frequencies up to 39 h^{-1}.[13] Very recently, while exploring the alkoxycarbonylation of alkenes with FA, Beller *et al.* discovered that palladium complexes, supported by chelating bis-phosphines decorated with pyridine bases, could catalyze the acceptorless decarbonylation of FA.[14] Because the dehydrogenation of HCOOH is facile, both thermodynamically and kinetically, the authors noted the concomitant release of at least 10% CO_2 and H_2. In the pursuit of a practical system able to selectively decarbonylate FA, we sought a metal-free method. Under organocatalytic conditions, the dehydrogenation of HCOOH is indeed difficult and only a handful of catalysts have been shown to decompose FA to CO_2 and H_2.[15] Herein, we report a system, combining a chemical looping and an organocatalytic transformation, for the decomposition of FA to CO and H_2O, without formation of H_2, at low temperature (<75 °C).

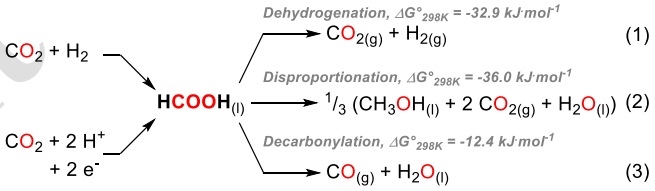

Scheme 1. Routes for the production and decomposition of formic acid.

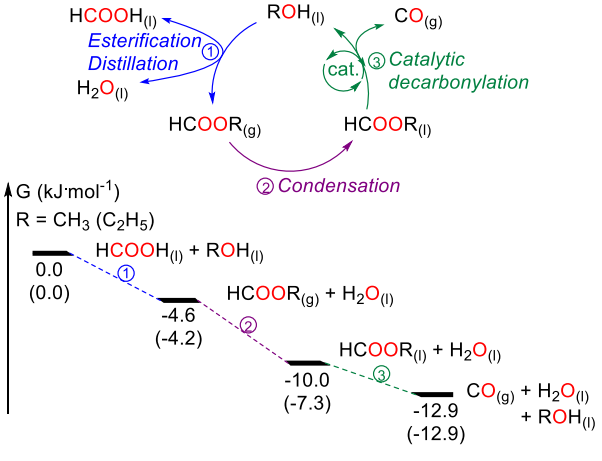

Scheme 2. Principle of a liquid chemical looping for the metal-free decarbonylation of formic acid, with the associated Gibbs free energies using methanol and ethanol as looping reagents.

From a mechanistic standpoint, the decarbonylation of FA must involve a C–H activation step that results in the formal deprotonation of the C–H group, to reduce the carbon atom.

[a] A. Imberdis, Dr. G. Lefèvre, Dr. T. Cantat
NIMBE, CEA, CNRS, Université Paris-Saclay, CEA Saclay 91191
Gif-sur-Yvette cedex, France
Fax: (+33) 1.6908.6640
E–mail: thibault.cantat@cea.fr

Computationally, the corresponding proton has a pKa of ca. 31.[16] The direct decarbonylation of HCOOH with an organic Brønsted base is hence illusory, in the presence of the more acidic O–H functionalities of FA (pKa = 3.7) or water. To circumvent this limitation, we envisioned a chemical looping strategy. Chemical looping is a powerful and practical approach where a transformation is divided into several sub-reactions to separate gases, prevent deleterious equilibria, and/or avoid incompatible substrates. It has been applied, using solid looping agents, in a variety of processes including the RWGS reaction, the (super-)dry reforming of methane and CO_2 capture from combustion.[17] An esterification reaction is well-suited to separate the acidic O–H functionalities from the C–H bond in Eqn. (3) because it would yield an alkylformate derivative with a Gibbs free energy intermediate between FA and CO + H_2O (Scheme 2). An alcohol was hence chosen to set up the chemical looping depicted in Scheme 2. It relies on the esterification of formic acid with an alcohol and isolation of the corresponding alkylformate by distillation (steps 1-2 in Scheme 2). The subsequent catalytic decarbonylation of the alkylformate would afford a stream of CO, while regenerating the alcohol. The choice of the best-suited looping agent is discussed at the end on this communication as it relies both on the physico-chemical properties of the alcohol/alkylformate couple and on the reactivity of the alkylformate in the decarbonylation step.

Interestingly, several metal catalysts have been reported for the acceptorless decarbonylation of alkylformates, based on copper[18a], ruthenium[18b], rhodium[18c], osmium[18d] and palladium[18e] complexes able to oxidatively add to the formate C–H bond. Organic alternatives exist, which involve guanidines[19], amines or phosphines.[20] All these catalysts nevertheless operate at elevated temperatures, above 140 °C. Reasoning that an alkoxide base (pKa = 29-32 in DMSO)[21] would be basic enough to deprotonate a C–H bond of a formate group, the fate of a DMF solution of methylformate (MF) was investigated, in the presence of 5.0 mol% potassium methoxide (MeOK). In a sealed NMR tube, a rapid decomposition of 56 % MF was noted, after 3 h at 19 °C in DMF (Entry 6, Table 1). The concomitant formation of methanol was observed by ^{1}H and ^{13}C NMR spectroscopy, while the production of CO was identified in the gas phase, using GC. Importantly, no H_2 nor CO_2 could be detected by GC, in the gas phase. A conversion of 85 % was reached at 75 °C, while no reaction occurred in the absence of the catalyst. Encouraged by this success, the influence of the nature of the catalyst, the solvent and the alkylformate were investigated (Table 1). Given the low exergonicity of the decarbonylation of MF ($\Delta G°_{298K}$= –2.9 kJ·mol^{-1}), the reaction operates under an equilibrium and, in a sealed NMR tube, a maximum conversion of 60 % was evaluated for the decomposition of MF *vs* 90 % at 75 °C, in agreement with an endothermic reaction ($\Delta H°_{298K}$= +36.9 kJ·mol^{-1}). A screening of solvents revealed that the decarbonylation of MF was efficient in polar, aprotic solvents having large dissociation constants, such as DMF (ε=36.7) and NMP (ε=32.2), with a conversion to CO and methanol of 56 and 58 %, respectively, after 3 h at 19 °C (see SI, Table S1). Importantly, the decarbonylation was completely shut down in methanol and in neat conditions, thereby showing the potential poisoning or deactivation of the catalyst by both the product and the substrate.

Table 1. Scope of the reaction for the decarbonylation of alkyl formate[a]

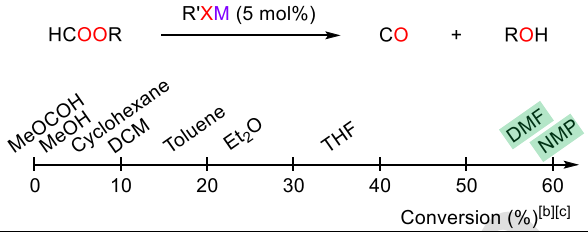

Entry	R	R'XM	T (°C)	Time (h)	Conv (%)[c]
1	Me	None	30	20	<5
2		MeOLi	30	8	54
3		MeONa	19	3	<5
4		MeONa/18C6	19	3	56
5		MeONa	30	3	46
6		MeOK	19 (75)	3	56 (85)
7		MeOK/18C6	19	3	47
8		MeOK/222	19	3	49
9		MeORb	19	3	44
10		EtOK	19	3	45
11		tBuOK	30	3	59
12		Me_2NLi	19	20	42
13		TBDNa	30	3	56
14		TBDK	19	4	50
15	Et	MeOK	19 (75)	2	24 (77)
16		EtOK	19	1	51
17	*n*Bu	tBuOK	30 (75)	3	60 (81)
18	Bz	MeOK	19 (75)	3	69 (94)

[a] Reaction conditions: 1 mmol MF, 50 µmol catalyst (5 mol%), 500 µL DMF. [b] Screening of the solvent (see details in the supporting information). [c] Determined by ^{1}H NMR of the crude reaction mixture.

While MeOLi and MeONa were found inactive at 19 °C, these catalysts decompose MF to CO and methanol at 30 °C and a longer reaction time was required in the presence of the lithium derivative (8 *vs* 3 h) (Entries 2, 3 and 5 in Table 1). The rubidium salt MeORb exhibited a catalytic activity close to MeOK (Entry 9 in Table 1). As alkali cations have been shown to influence the performances of catalytic systems by coordination to oxygen-rich substrates, the coordination sphere of the potassium cation in MeOK was modulated by the addition of exogenous chelating ligands. Addition of 5.0 mol% of the 18–C–6 crown ether or the 2,2,2-cryptand had no impact on the catalytic performances of MeOK, suggesting an innocent role of K^+. The difference in reactivity between MeOK and its lithium and sodium congeners hence likely stems from the tighter ion pairs formed between the MeO^- anion and the hard Li^+ and Na^+ cations. This trend is reflected in the shortening of O–M bond length in the alkali oxides M_2O from 2.9, 2.8, 2.4 to 2.0 Å across the series Rb, K, Na, Li.[22] This interpretation is supported by the comparable catalytic activities of MeOK and MeONa/18–C–6 at 19 °C (Entries 4 and 6 in Table 1). It is notable that bases stronger than MeOK, such as EtOK, *t*-BuOK and nitrogen-containing bases (TBDK), exhibited

catalytic performances similar to MeOK; similarly, Me_2NLi behaved like MeOLi.

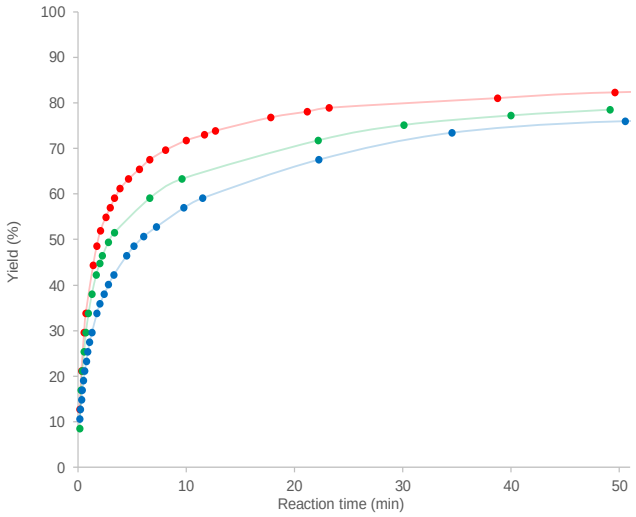

Figure **1.** Plot of the volume of CO produced upon decarbonylation of methyl formate in an open system using different initial loadings of MeOH (red: 0 mol% MeOH, green: 5 mol% MeOH, blue: 10 mol% MeOH) and evolution of the rate constant with respect to the initial concentration of MeOK and MeOH.

Bulkier ethyl and *n*-butyl formates were found to be less reactive than MF and required stronger bases as catalysts (entries 15-17). In contrast, 94 % of the more activated benzyl formate was decomposed at 75 °C. It is noteworthy that all the results displayed in Table 1 involved very mild temperatures (19°C or 30°C).

To suppress the thermodynamic constraint associated with pressure buildup in a closed vessel, the decomposition of MF was carried out in an open system and monitored using a eudometer (Figure 1). Using the reaction conditions of Entry 6, Table 1, CO was generated in 82 % yield after only 50 min at 19 °C (red plot in Figure 1). The setup enabled a kinetic study, establishing that the rate law is first order in catalyst and has a -1 order in MeOH while the order for MF is non-integer (SI).

These data confirm that both MF and MeOH have a detrimental effect on the reactivity of the catalyst and, to better apprehend this behavior, DFT calculations were carried out on the mechanism of the decarbonylation reaction.

The MeO^- catalyst is a base strong enough to interact with MF and, although the deprotonation of the C–H bond is slightly uphill (ΔG = +5.1 kcal.mol^{-1}), CO release occurs readily *via* a low lying transition state (TS_2, ΔG = +8.1 kcal.mol^{-1}) (Scheme 3, green surface). Interestingly, the methanol by-product forms a strong H-bond with MeO^- and the separation of the free MeO^- base from methanol requires +7.3 kcal.mol^{-1}. As a result, the energy span governing the activity of the MeO^- catalyst reaches 15.4 kcal.mol^{-1}.

As the reaction proceeds, the accumulation of methanol can be accounted for, mechanistically, by exploring the catalytic behavior of the H-bonded [MeO^-···HOMe] pair (blue surface in Scheme 3). The decreased basicity of the catalyst results in a destabilization of the two transitions states responsible for the deprotonation of the C-H bond in MF and the release of CO from the $CH_3OC(O)^-$ anion (e.g. TS_2, ΔG = +14.5 kcal.mol^{-1}). As a consequence, in the presence of methanol, the reaction span increases to 19.8 kcal.mol^{-1}, thereby explaining the deleterious influence of the reaction product on the catalyst activity. In addition, the presence of a large excess MF results in the trapping of the MeO^- catalyst to form a $HC(OMe)_2O^-$ anion (with a Gibbs free energy of –3.7 kcal.mol^{-1}), thereby slowing down the rate of the decarbonylation.

Based on these key findings, an optimized system was found for the decarbonylation of formic acid, using the chemical looping depicted in Scheme 2. MeOH/MF was selected as the best looping system, because both MeOH and MF are liquids under ambient conditions and MF presents a high CO content of 47 wt%. Using a two-chamber system depicted in Scheme 4, a solution of MeOK in DMF (0.07 mol/L) was connected to a vessel containing pure MF. The device was equipped with a condenser and immersed in a 75°C oil bath. Thanks to the low boiling-points of

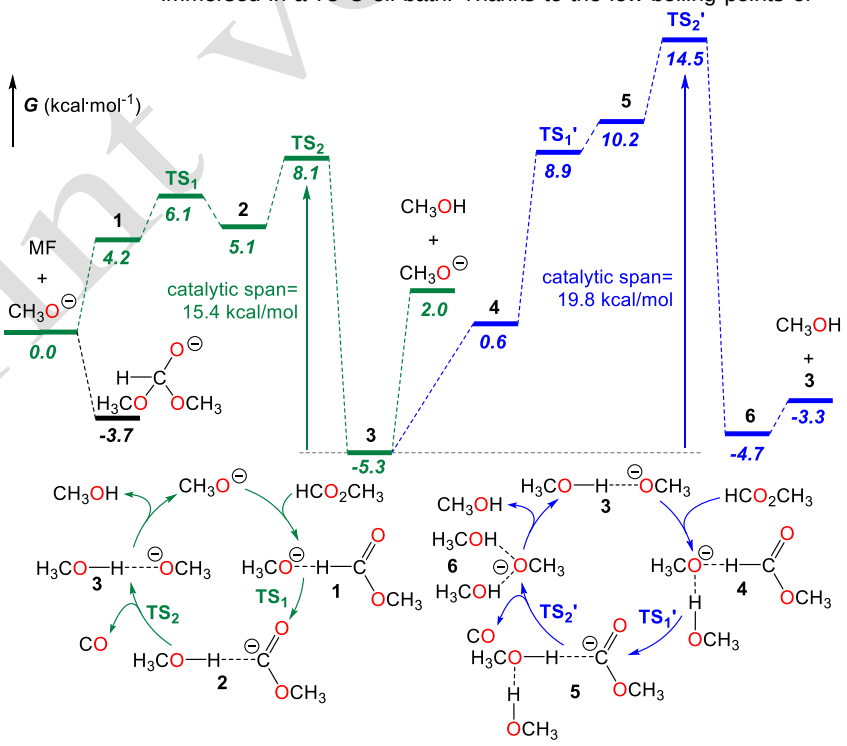

Scheme 3. Decarbonylation of methyl formate catalyzed by MeO^-.Gibbs free energies in kcal.mol^{-1} computed at the M062x/6-311++G**/PCM level of theory.

MF and MeOH of 32 and 61 °C, respectively, the accumulation of the reagents and products in the solution containing the catalyst (chamber B in Scheme 4) is avoided and methanol is collected in the reservoir vessel (chamber A). Using this setup, an excellent TON of 5000 was measured, with a TOF up to 81 h^{-1} at 75 °C. Overall, 10 mL MF were successfully decarbonylated in 92 % yield to afford 3.7 L CO, after 40 h (Scheme 4). 6.1 mL of

methanol were recovered, with a purity of 96 % (along with 4 % unreacted MF). To demonstrate the liquid chemical looping depicted in Scheme 2, the regeneration of MF was carried out by esterification of the produced methanol with HCOOH at 32 °C. Continuous distillation of MF enabled the isolation of the alkylformate in 86 % yield after 5 h, thanks to the absence of azeotrope between MF and formic acid, water or methanol.

Scheme 4. Catalytic decarbonylation of MF using a two-chamber setup [a]

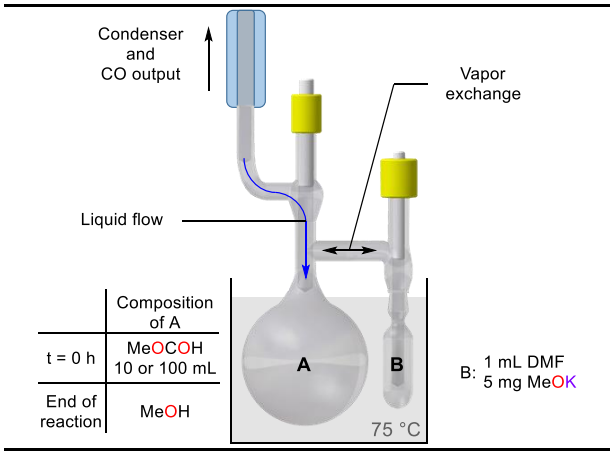

Entry	Reagent (mL / mol)	Time	TON[b]	TOF (h^{-1})[b]	Yield (%)[b]
1	MeOCOH 10 / 0.16	20 h	1618	81	70
2	MeOCOH 10 / 0.16	40 h	2171	54	92
3	MeOCOH 100 / 1.6	4 d	5000	52	22

[a] Reaction conditions: In a two-chamber system surmounted with a cooler, pure MF is introduced in the reserve chamber (A) and the catalytic chamber (B) is charged with 7 µmol catalyst (5 mg) and 1 mL DMF. The setup is immersed in an oil bath at 75 °C. [b] Determined by ^{1}H NMR of an aliquot of compartment A mixture.

All together, the decarbonylation of formic acid to CO and water was achieved in 79 % yield at low temperature (75 °C), using metal-free catalysts, for the first time (Scheme 5). No H_2 nor CO_2 contamination of the gas stream was detected by GC, although the dehydrogenation of formic acid is thermodynamically preferred.

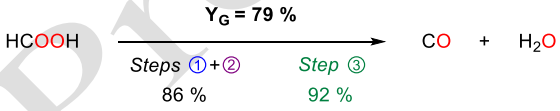

Scheme 5. Global process (Y_G = global yield of the process)

Recently, several surrogates of CO have been designed to generate low pressures of CO for synthesis at the laboratory scale, for instance using two-chamber systems (e.g. COgen).[23] Similarly, we were able to perform the gram-scale aminocarbonylation of 4-bromoanisole with morpholine, using CO produced from MF (Scheme 6).[24] The absence of H_2 circumvented the dehalogenation of the arylbromide in this palladium-catalyzed reaction. Interestingly, the possibility to generate high pressures of CO (up to 26 bars), allowed the iron-catalyzed carbonylation of the N–CH_3 bond in N,N-dimethylaniline in 73 % yield under 9 bars of CO, using a double autoclave system (see SI, Scheme 6).[25] While chemical loopings are common strategies in the realm of heterogenous catalysis, the present work hence exemplifies how liquid chemical loopings can unlock thermodynamically unfavored transformations, at low temperatures, without the need for sophisticated metal catalysts.

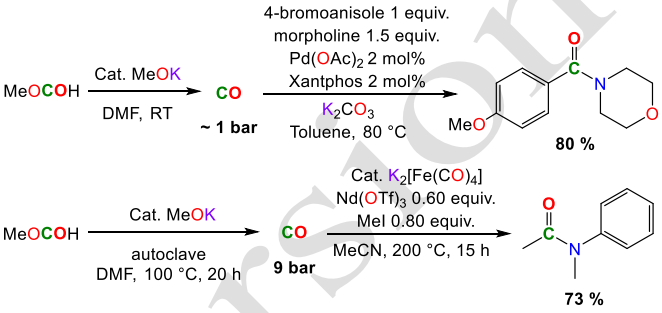

Scheme 6. Tandem carbonylation reactions enabling the preparation of amides with CO generated from MF.

Acknowledgements

The authors acknowledge for financial support of this work: CEA, CNRS, CINES (project sis6494), the CHARMMMAT Laboratory of Excellence, and the European Research Council (ERC Consolidator Grant to T.C.).

Keywords: Formic acid; CO; organocatalysis; mechanisms

[1] a) S. Wesselbaum, V. Moha, M. Meuresch, S. Brosinski, K. M. Thenert, J. Kothe, T. vom Stein, U. Englert, M. Hölscher, J. Klankermayer, et al., *Chem. Sci.* **2015**, *6*, 693–704. b) M. Behrens, F. Studt, I. Kasatkin, S. Kuhl, M. Havecker, F. Abild-Pedersen, S. Zander, F. Girgsdies, P. Kurr, B.-L. Kniep, et al., *Science*. **2012**, *336*, 893–897.

[2] a) A. S. Agarwal, Y. Zhai, D. Hill, N. Sridhar, *ChemSusChem* **2011**, *4*, 1301–1310. b) C. Federsel, R. Jackstell, M. Beller, *Angew. Chemie Int. Ed.* **2010**, *49*, 6254–6257. c) C. Federsel, C. Ziebart, R. Jackstell, W. Baumann, M. Beller, *Chem. Eur. J.* **2012**, *18*, 72–75.

[3] a) A. J. M. Miller, D. M. Heinekey, J. M. Mayer, K. I. Goldberg, *Angew. Chemie Int. Ed.* **2013**, *52*, 3981–3984. b) S. Savourey, G. Lefèvre, J.-C. Berthet, P. Thuéry, C. Genre, T. Cantat, *Angew. Chemie Int. Ed.* **2014**, *53*, 10466–10470. c) M. C. Neary, G. Parkin, *Chem. Sci.* **2015**, *6*, 1859–1865. d) K. Sordakis, A. Tsurusaki, M. Iguchi, H. Kawanami, Y. Himeda, G. Laurenczy, *Green Chem.* **2017**, *19*, 2371–2378. e) A. Tsurusaki, K. Murata, N. Onishi, K. Sordakis, G. Laurenczy, Y. Himeda, *ACS Catal.* **2017**, *7*, 1123–1131.

[4] a) A. Boddien, F. Gärtner, C. Federsel, P. Sponholz, D. Mellmann, R. Jackstell, H. Junge, M. Beller, *Angew. Chemie Int. Ed.* **2011**, *50*, 6411–6414. b) K. Sordakis, C. Tang, L. K. Vogt, H. Junge, P. J. Dyson, M. Beller, G. Laurenczy, *Chem. Rev.* **2018**, *118*, 372–433.

[5] T. Zell, R. Langer, *Phys. Sci. Rev.* **2018**, *3*, 57-93.

[6] J. H. Jones, *Platin. Met. Rev.* **2000**, *44*, 94–105.

[7] I. Dybkjaer, *Fuel Process. Technol.* **1995**, *42*, 85–107..

[8] F. D. Doty, G. N. Doty, J. P. Staab, L. L. Holte, **2010**, 1–10.
[9] a) J. Klankermayer, S. Wesselbaum, K. Beydoun, W. Leitner, Angew. Chemie Int. Ed. **2016**, *55*, 7296–7343. b) W. Supronowicz, I. A. Ignatyev, G. Lolli, A. Wolf, L. Zhao, L. Mleczko, Green Chem. 2015, 17, 2904–2911.
[10] a) X. Qi, C.-L. Li, X.-F. Wu, *Chem. - A Eur. J.* **2016**, *22*, 5835–5838. b) F.-P. Wu, J.-B. Peng, X. Qi, X.-F. Wu, *Catal. Sci. Technol.* **2017**, *7*, 4924–4928. c) J.-P. Simonato, *J. Mol. Catal. A Chem.* **2003**, *197*, 61–64. d) T. G. Ostapowicz, M. Schmitz, M. Krystof, J. Klankermayer, W. Leitner, *Angew. Chemie Int. Ed.* **2013**, *52*, 12119–12123.
[11] J. S. Morgan, *J. Chem. Soc., Trans.* **1916**, *109*, 274–283.
[12] W. L. Nelson, C. J. Engelder, *J. Phys. Chem.* **1925**, *30*, 470–475.
[13] P. Losch, A. S. Felten, P. Pale, *Adv. Synth. Catal.* **2015**, *357*, 2931–2938.
[14] R. Sang, P. Kucmierczyk, K. Dong, R. Franke, H. Neumann, R. Jackstell, M. Beller, *J. Am. Chem. Soc.* **2018**, *140*, 5217–5223.
[15] C. Chauvier, A. Tlili, C. Das Neves Gomes, P. Thuéry, T. Cantat, *Chem. Sci.* **2015**, *6*, 2938–2942.
[16] The pKa-values were calculated with respect to the furan anion as reference base (experimental value of 35) according to the formula: $pKa(THF)$ = 35 + ΔG/(2.303∗R∗T) (ΔG in kcal.mol^{-1} and T in K); K. Shen, Y. Fu, J.-N. Li, L. Liu, Q.-X. Guo, *Tetrahedron Lett.* **2007**, *63*, 1568-1576.
[17] a) M. Keller, J. Fung, H. Leion, T. Mattisson, *Fuel* **2016**, *180*, 448–456. b) M. Wenzel, L. Rihko-Struckmann, K. Sundmacher, *Chem. Eng. J.* **2018**, *336*, 278–296. c) T. Pröll, P. Kolbitsch, J. Bolhàr-Nordenkampf, H. Hofbauer, *AIChE J.* **2009**, *55*, 3255–3266. d) M. Ryden, A. Lyngfelt, *Int. J. Hydrogen Energy* **2006**, *31*, 1271–1283. e) M. M. Hossain, H. I. de Lasa, *Chem. Eng. Sci.* **2008**, *63*, 4433–4451.
[18] a) G. Doyle, US Pat., **1981**, 4.319.050. b) G. Jenner, E. M. Nahmed, H. Leismann, *Tetrahedron Lett.* **1989**, *30*, 6501–6502. c) H. A. Zahalka, H. Alper, *Tetrahedron Lett.* **1987**, *28*, 2215–2216. d) C. Legrand, Y. Castanet, A. Mortreux, F. Petit, *Tetrahedron Lett.* **1992**, *33*, 3753–3756. e) J. S. Lee, J. C. Kim, Y. G. Kim, *Appl. Catal.* **1990**, *57*, 1–30.
[19] M. J. Green, Eur Pat., **1984,** *EP0115387*.
[20] F. R. Vega, J. C. Clément, H. des Abbayes, *Tetrahedron Lett.* **1993**, *34*, 8117–8118.
[21] W. N. Olmstead, Z. Margolin, F. G. Bordwell, *J. Org. Chem.* **1980**, *45*, 3295–3299.
[22] N. K. McGuire, M. O'Keeffe, *J. Solid State Chem.* **1984**, *54*, 49–53.
[23] a) C. Veryser, S. Van Mileghem, B. Egle, P. Gilles, W. M. De Borggraeve, *React. Chem. Eng.* **2016**, *1*, 142–146. b) C. Veryser, G. Steurs, L. Van Meervelt, W. M. De Borggraeve, *Adv. Synth. Catal.* **2017**, *359*, 1271–1276. c) S. D. Friis, A. T. Lindhardt, T. Skrydstrup, Acc. Chem. Res. 2016, 49, 594–605.
[24] J. R. Martinelli, D. A. Watson, D. M. M. Freckmann, T. E. Barder, S. L. Buchwald, J. Org. Chem. **2008**, *73*, 7102–7107.
[25] T. Nasr Allah, S. Savourey, J.-C. Berthet, E. Nicolas, T. Cantat, Angew. Chemie Int. Ed. **2019**, *58*, 10884–10887.